Quasielastic Light Scattering

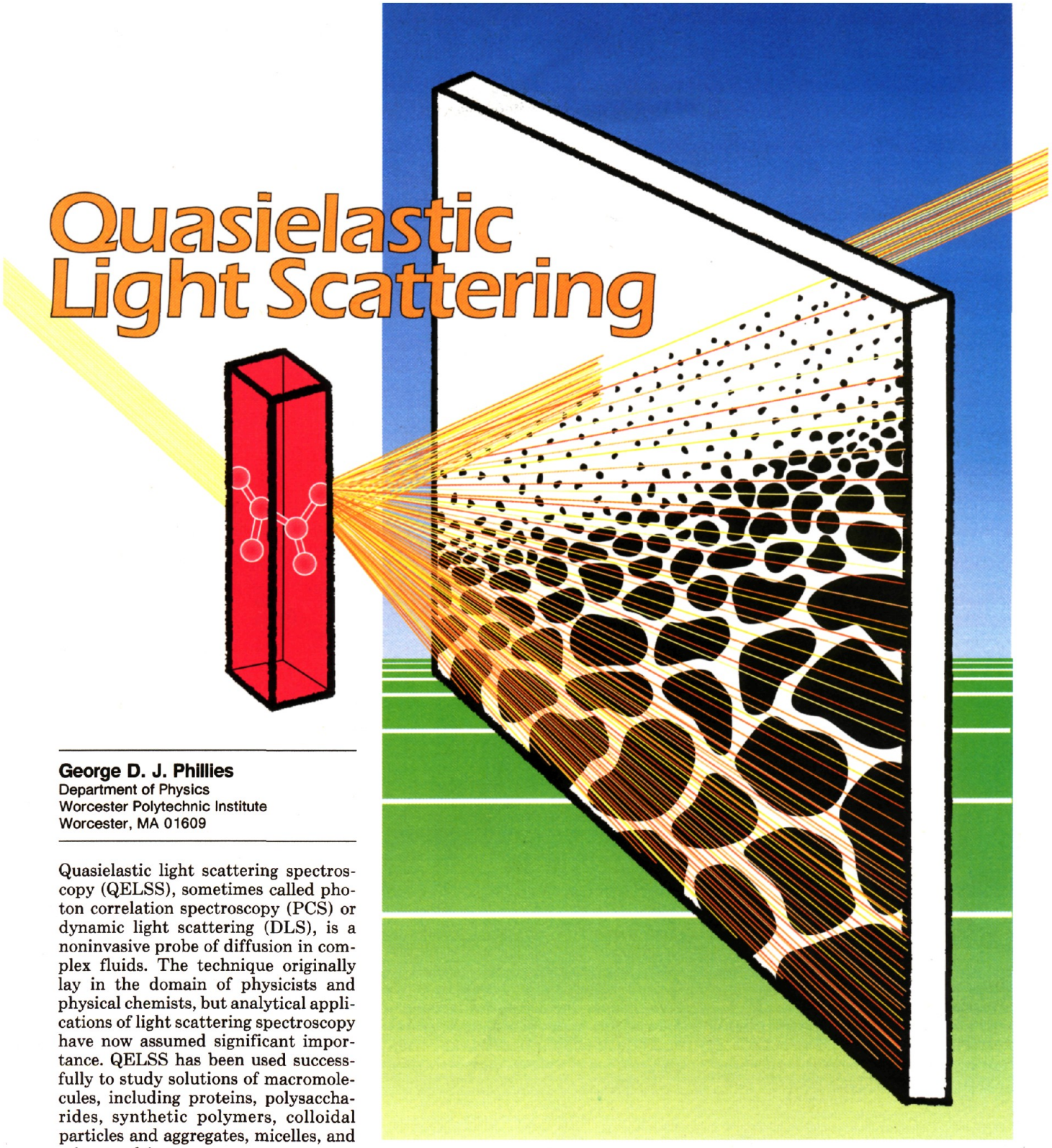

George D. J. Phillies
Department of Physics
Worcester Polytechnic Institute
Worcester, MA 01609

Quasielastic light scattering spectroscopy (QELSS), sometimes called photon correlation spectroscopy (PCS) or dynamic light scattering (DLS), is a noninvasive probe of diffusion in complex fluids. The technique originally lay in the domain of physicists and physical chemists, but analytical applications of light scattering spectroscopy have now assumed significant importance. QELSS has been used successfully to study solutions of macromolecules, including proteins, polysaccharides, synthetic polymers, colloidal particles and aggregates, micelles, and microemulsions.

In most cases, light scattering spectroscopy yields directly the mutual diffusion coefficient of the scattering species. When applied to dilute, monodisperse solutions, the diffusion coefficient obtained by QELSS can be used to estimate the size (and hence the molecular weight) of macromolecules in solution. With polydisperse systems, light scattering spectroscopy successfully estimates the width of molecular weight distributions.

The dominant practical application of QELSS is in particle sizing. With a dilute monodisperse preparation, light scattering provides a reproducible, rapid (5–30 min), accurate procedure for measuring particles ranging from 5 nm to 5 μm in solution. Because QELSS is a noninvasive, nondestructive technique, artifacts associated with particle isolation, sample drying, and sample loss can be avoided.

In this article we will present a largely nonmathematical treatment of light scattering spectroscopy, stressing analytical applications. For additional information, readers are referred to recent review articles and monographs

0003-2700/90/A362-1049/$02.50/0

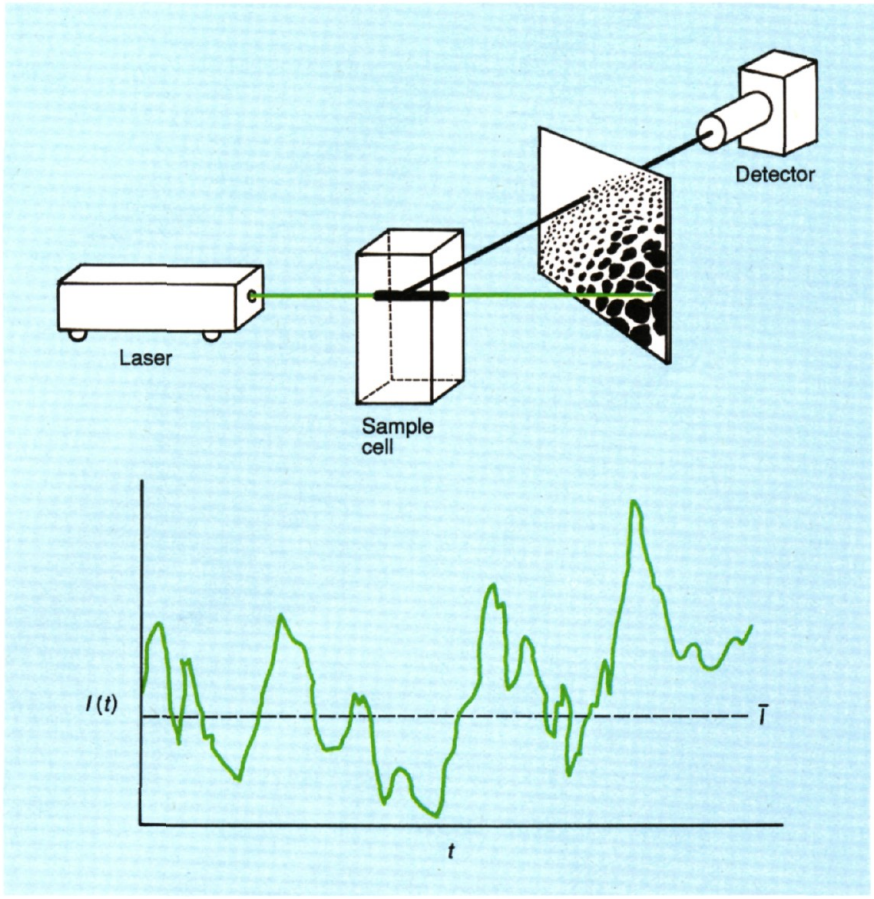

Figure 1. Typical light scattering apparatus.

Laser light falls on the sample cell, the sample scattering light in all directions. Under favorable conditions, a white card placed obliquely to the laser beam can be used to visualize the scattered light. If light scattered in a single direction is observed, a recording of the detector output (scattering intensity) $I(t)$ as a function of time (lower half of figure) shows that $I(t)$ fluctuates randomly around its average $\bar{I}$. (Adapted with permission from Reference 2.)

(*1–10*). Because QELSS bears little semblance to techniques that are commonly covered in undergraduate or graduate curricula, fundamental physical issues as well as limitations and artifacts will be discussed.

Begin with a simple picture of a light scattering spectrometer (Figure 1). In a conventional instrument, a monochromatic laser source illuminates the sample cell. The sample, typically a macromolecule solution or macroparticle suspension in analytical work, scatters some laser light in each direction. If the sample cell is viewed from the side (taking appropriate precautions against direct viewing of the laser beam or its reflections), the scattered light is visible to the naked eye. When the scattered light is projected onto a card, it appears as a constellation of bright and dark patches (each of which is a "coherence area") that flicker and glimmer randomly in time.

A quantitative record of the fluctuating intensity $I(t)$ of the light scattered through a small range of directions (i.e., $I(t)$ of the light scattered into a small number of coherence areas) can be obtained with an iris and a photodetector, as indicated in the figure. The flickering effect, which results from the Brownian motion of solute macromolecules, occurs in samples that have come to thermal equilibrium. Unlike classical gradient diffusion measurements, which require the experimenter to prepare a nonequilibrium system containing regions of different solute concentration, diffusion measurements using QELSS are performed on gradient-free equilibrium solutions that usually can be prepared with simple filtration procedures.

A record of $I(t)$ can be used to find the average intensity, $\bar{I}$. In a classic static scattering experiment (light scattering photometry), $\bar{I}$ is used to construct Zimm plots, as discussed by Cantor and Schimmel (*11*). Under favorable conditions Zimm plots reveal the z-average molecular weight (the average molecular weight of all scattering species, the average being weighted by the intensity of the light scattered by each species), the second virial coefficient (a measure of the thermodynamic nonideality of a solution), and the radius of gyration (the mean square distance measured from the center of mass of the scattering macromolecule to each of the macromolecule's component parts) (*7, 8, 11*). In light scattering spectroscopy, the interest lies not in $\bar{I}$ but in the intensity fluctuation $\delta I(t) = \bar{I}(t) - I$; the time dependence of $\delta I(t)$ is determined by molecular transport properties. Light scattering spectroscopy and light scattering photometry use precisely the same photons. The experiments differ only in how $I(t)$ is analyzed after being detected, so photometry and spectroscopy may be done simultaneously with a single piece of equipment.

In the following sections, the source, temporal evolution, and characterization of light scattering intensity fluctuations as well as the interpretation of QELSS spectra will be presented.

Physical basis of light scattering

Figure 1 indicates that the scattering intensity in each direction fluctuates. A full mathematical treatment of light scattering must recognize that the sample contains some large number N ($\sim 10^{10}$–10^{12}) of scattering centers. However, the physical events that are significant for light scattering occur in a system that contains only two scattering centers (Figure 2).

In this figure, the two hashed lines represent light propagating from a source to scatterers to a detector. If the two beams of light arrive at the detector in phase with each other, there will be constructive interference between the waves. That is, if the wave crests of each beam of light are aligned with the wave crests of the other beam of light, the waves will add together positively; the sum of the waves will be large, so the detected light will be bright. If the two beams of light arrive out of phase with each other, there will be destructive interference. That is, if the wave crests of each beam are aligned with the wave troughs of the other beam, the two waves will tend to cancel each other out; the sum of the waves will be small, so little light will be detected. In the figure, the two light paths are unequal and differ by a fractional number of waves, so scattering from the two particles leads to destructive interference at the detector.

In a real system, the intensity $I(t)$ of light scattered sideways out of the incident laser beam is determined by the brightness and relative phase of light scattered by each of the N^2 pairs of particles. If a solution were totally ho-

mogeneous on a microscopic scale, then the detector would receive equal amounts of scattered light having each possible phase. If one combines equal amounts of light of every phase, total destructive interference occurs at the detector; the scattered intensity vanishes.

Light scattering is seen from physical samples because equilibrium solutions are not completely homogeneous. Brownian motion moves solute molecules in a quasi-random manner, so that the numbers n_1, n_2, ... of solute molecules in a series of adjacent sample volumes will almost never be equal to each other. The light scattered from a series of adjacent volumes, besides differing in phase from volume to volume, therefore also differs in amount. In scattering from a real system, the amount of light reaching the detector is thus different for each possible phase, so destructive interference between light of different phases is not total. Brownian motion—thermal concentration fluctuations—leads to light scattering by equilibrium samples.

Brownian motion (particle diffusion) causes the solute molecules to move. When the particles change positions, the light paths (and hence the phases) of the scattered waves are altered. If the phases of the scattered rays change, the system drifts between constructive and destructive interference between the scattered rays, and the detected intensity fluctuates between bright and dim.

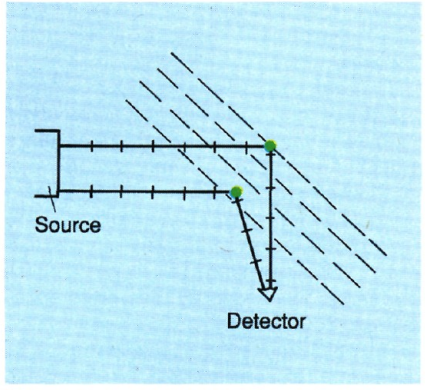

Figure 2. Interference effects in light scattering.

Coherent light, emitted by the laser, is scattered by each of two solute particles (green circles), eventually reaching the detector. Hash marks on the light paths represent points of equal phase of the laser light. All light paths begin at the laser with the same phase. Because different paths have different lengths, light scattered by different particles reaches the detector with different phases, resulting in interference. Diagonal dashed lines represent planes of constant phase, and all particles lying on any of the indicated planes scatter light that reaches the detector with a single phase. (Adapted with permission from Reference 2.)

Light scattering spectroscopy involves the time scale of these diffusion-driven intensity fluctuations. To transform Figure 2 from a figure that shows destructive interference to one that shows constructive interference, the particles must diffuse far enough that the two indicated light paths change their relative lengths by roughly half a light wavelength. The typical time, τ, required for such a diffusion step is

$$\tau^{-1} = D\,k^2 \qquad (1)$$

where τ provides a natural time scale for the experiment. D is the translational (mutual) diffusion coefficient of the solute species, and k is the magnitude of the scattering vector **k**, expressed as

$$k = \frac{4\pi n}{\lambda} \sin(\theta/2) \qquad (2)$$

where θ is the scattering angle, with forward scattering at 0° and right-angle scattering at 90°; n is the index of refraction of the solution; and λ is the laser wavelength measured in vacuo. Experimental determination of τ allows calculation of the diffusion coefficient.

Intensity fluctuations may also be described in terms of the Doppler effect. (One must be careful with mathematical details, however, because solute molecules do not move in straight lines or at constant speed.) In essence, the incident laser beam is at a single frequency, ω_0. Light, when scattering from a moving macromolecule, changes its frequency. Because different macromolecules move in different directions with different speeds, the scattered light gains a range of frequencies $\omega_0 \pm \delta\omega$ centered on ω_0. On detection, "beat notes" between rays of light scattered with different frequencies become apparent. These beat notes are seen as fluctuations in the scattered intensity having frequencies $\sim 2\,\delta\omega$, the "2" appearing because frequency changes can move the scattered light up or down in frequency from the incident frequency.

How does the time scale τ manifest itself in the scattering intensity? Consider $I(t)$, plotted against t (Figure 1). $I(t)$ is a random function of time. There are moments t_1, t_2, ... when $I(t)$ is especially large. The behavior of $I(t_i + \delta t)$, subsequent to moments t_i when $I(t)$ was large, differs from one t_i to the next. With one initial moment t_1, $I(t)$ may fall as time goes on. With a different initial moment t_2, $I(t)$ may increase with time. However, if at t_i the scattering intensity was especially large, on the average as time passes the scattering intensity decays exponentially back to its average value, $\bar{I}$.

One could construct an instrument that waited for moments when $I(t)$ had a specific large value, made records of $I(t + \delta t)$ for a series of moments t, and computed the average behavior of $I(t + \delta t)$ from all the records. Such devices have actually been built; they are adequate for approximate measurements in systems with high signal-to-noise ratios (S/N). A more efficient approach is to use the recorded $I(t)$ to compute

$$C(\delta t) = \int_0^T dt I(t) I(t + \delta t) \qquad (3)$$

where T is the duration of the experiment and $C(\delta t)$ is the intensity–intensity autocorrelation function ("the correlation function" for short) of the scattered light. $C(\delta t)$ is a weighted average of $I(t + \delta t)$, and the weighting factor in the average is the initial intensity $I(t)$. An instrument that processes $I(t)$ into $C(\delta t)$ is a (digital) correlator—the "digital" referring to the use of integer–arithmetic logic circuits, rather than analog circuits, to compute $C(\delta t)$.

Apparatus considerations

Several light scattering spectrometers are commercially available as complete units (often described as "particle sizers") and as major components. Here we note issues of importance to those who might wish to assemble or modify equipment or to identify an instrument suitable for a specific application. Ford (*12*) gives an excellent review of equipment design issues.

The only suitable light source for a QELSS apparatus is a stable, monochromatic, polarized CW laser. There is no advantage in most experiments to single-moding the laser with a cavity etalon; indeed, single-moding can reduce laser power and hence spectrum quality. The signal in classic light scattering photometry scales with the illuminating wavelength as λ^{-4}, encouraging the use of blue-violet light sources in photometry. In a QELSS experiment, S/N is determined by the number of photons detected per correlation time τ in a single diffraction-limited coherence area; thus, for QELSS, the S/N scales as λ^{+1} (*1*). Most detectors are less effective at longer wavelengths, so under practical conditions changing the laser wavelength has little effect on QELSS spectral quality. To enhance the signal, it is far more effective to increase the beam brightness than it is to change the wavelength.

For almost all analytical applications, including most studies of polymer, protein, biomacromolecule, and micelle systems, a minimum available laser power of 200–500 mW is mandatory. Conventional Ar^+ and Kr^+ gas lasers are widely used. The medium-power (10–30 mW) He–Ne laser is ade-

quate for sizing some particulates but is not suitable for rapid measurements on most of the more weakly scattering systems. The ubiquitous polystyrene latex (PSL) sphere suspensions, often used to demonstrate the efficacy of light scattering spectrometers, scatter light far more efficiently than almost any interesting system does. The capability of an instrument to size PSL suspensions is no indication that the instrument is suitable for most real analytical applications.

Although even very small Ar^+ lasers yield 250 mW on one line, realistically (assuming regular mirror and prism cleaning and walking of the plasma tube) over the life of the plasma tube the power output does not always achieve nominal specifications. By using a somewhat larger laser, difficulties that result from apparatus aging may be avoided. We have found 3–4 W (all lines) Ar^+ systems to be adequate for most purposes. In selecting a laser, an important consideration is that the light output be rigorously free of coherent (single frequency) ripple. Such a ripple, often found either at a multiple of the power line frequency (50 or 60 Hz) or at an rf drive frequency (50–100 kHz), is a disaster for a light scattering spectrometer because the autocorrelation process amplifies even weak coherent noise into a dominant, meaningless feature of the spectrum.

To compute $I(t)I(t + \delta t)$ one needs at least two photons, one received at t and the other at $t + \delta t$. QELSS is thus a two-photon process. In light scattering spectroscopy, the measured S/N therefore depends on the brightness (power/area) of the incident beam inside the sample cell, not on the absolute power of the input laser. A weak laser with a tightly focused beam can give a better spectrum than a powerful laser with poor focusing.

Ford (*12*) has given definitive arguments showing that rectangular scattering cells are preferable to cylindrical cells, especially for multiangle work, although cylindrical cells and a well-designed optical train will give good results. The only substantial argument in favor of cylindrical cells is that they simplify index of refraction/scattering angle corrections. These corrections arise because the angle θ appearing in Equation 2 is the angle measured in solution inside the sample cell, not the refraction-modified angle readily measured on the optical table outside the sample cell. The relevant correction involves Snell's law. Although cylindrical cells are readily aligned with the incident laser beam, they are difficult to align adequately with the optical train of the detector, as Ford describes (*12*). Cells need not be large; Foord et al. (*13*) have demonstrated the use of melting point capillaries to make measurements with microscale (microliter) samples.

The appropriate detector for a light scattering spectrometer is a photomultiplier tube (or equivalent) linked to photon-counting electronics. The primary figure of merit for a phototube, in a QELSS experiment, is its limiting photocurrent: the largest number of photons that the tube can count continuously over sustained periods of time (hours to days) without entering a nonlinear regime (in which photocounts are lost or double-counted) or causing physical damage to the photocathode. The larger the limiting current, the more readily measurements can be made.

In typical QELSS experiments, count rates of 1×10^5 to 3×10^5 or more photons per second or larger are desirable. Limiting currents for some detectors optimized for Raman spectroscopy corresponding to 3×10^5 counts per second are sometimes quoted. Such limiting count rates are tolerable for the short times needed to scan through an intense Raman line, but prolonged exposure to these rates may damage the tube. A second important figure of merit for a tube is the quantum efficiency ϵ at the laser wavelength. A large ϵ is desirable, and for visible laser wavelengths a good photomultiplier tube will have an ϵ of 15–30%.

For measurements on macroparticles, large proteins, and large M polymers, the detector dark count (the signal produced by the phototube and electronics when no light is entering the system) is usually not important. With almost any phototube the dark noise is generally much weaker than the signal. A periscope that permits viewing of the scattering volume through a telescope from the direction from which that volume is seen by the detector can help to identify artifacts resulting from cell scratches, dust contamination in the sample, and so forth. Appropriate precautions need to be taken before viewing areas that are side-illuminated by laser radiation.

Correlator design is now well understood. In essence, a digital correlator breaks time into intervals $(t, t + \Delta t)$, $(t + \Delta t, t + 2\Delta t), \ldots, (t + (i - 1)\Delta t, t + i\Delta t)$ and counts the number n_i of photons detected in each interval i. The correlation function $C(t)$ is obtained operationally as a sum rather than an integral

$$C(m\Delta t) = \sum_{j=1}^{N-m} n_j n_{j+m} \qquad (4)$$

where Δt is the sample time or bin width, $m\Delta t$ is the delay time, and N is the duration of the experiment in units of the sample time. The circuitry that computes $C(m\Delta t)$ for one m is a channel; most correlators have 64, 128, or more channels. Channels need not be evenly spaced; that is, one need not choose $m = 1, 2, 3, 4, \ldots$. With polydisperse samples, a channel spacing that increases with channel number (e.g., $m = 1, 2, 3, \ldots, 64, 66, 68, \ldots, 128, 132, 136, \ldots$) can be helpful. Some correlator systems increase not only the channel spacing but also the bin width with increasing channel number, so that, for example, if $m = 64, 66, 68, \ldots$, then $C(66\Delta t) = \sum_{j=1}^{N-66} (n_j n_{j+65} + n_j n_{j+66})$. A few recent designs have used a small number of individually placed channels. Accurate spectral analysis requires knowledge of $C(\infty)$, which can be measured with delay channels set at times $M\Delta t$ for some large M.

Because correlators divide time into intervals of width Δt, they have an intrinsic time/frequency resolution limit. It is therefore impossible to measure $C(0)$ directly. Also, if $C(t)$ changes too rapidly with time, the measured $C(t)$ is not a good representation of the actual correlation function. A good rule of thumb for practical work is that $C(t)$ should not change by more than 50% in an interval $10\Delta t$. If the system is a mixture of widely different sizes of particle, this rule should be applied to the relaxation of the most rapidly moving particles. If $C(t)$ has been measured reliably over all significant time scales so that Δt is small enough and $M\Delta t$ is large enough to avoid artifacts, D calculated from $C(t)$ should be virtually independent of Δt.

Optical alignment can have a substantial effect on S/N. A common error of naive operators is taking a large number of mediocre spectra without realizing that experimentation should be postponed until efforts are made to improve S/N by realigning the optical train, remaking samples, or peaking up the laser power. Badly measured spectra often look qualitatively much like well-measured spectra; good and bad spectra differ primarily in the noise level.

Interpretation of spectra

The simplest spectra are obtained from dilute solutions of monodisperse, nearly spherical solutes such as polystyrene latex spheres or globular proteins. In these systems

$$C(t) = A \exp(-2Dk^2t) + B \qquad (5)$$

where A is the spectral amplitude and B is the baseline. Although B can be

calculated from the total number of photocounts P observed during a measurement that lasts N sample times, namely $B = P^2/N$, it is wiser to view B as an experimentally measurable quantity. Agreement between calculated and measured B can be considered a test that the apparatus is working correctly. With a truly monodisperse sample, the slope of a weighted linear least-squares fit of a straight line to log $(C(t) - B)$ yields D.

Light scattering spectra are directly sensitive to the translational diffusion coefficient D of the solutes. If the scatterers are substantially nonspherical, $C(t)$ contains terms reflecting the rotational diffusion coefficient D_r, as discussed by Berne and Pecora (*4*). For a dilute, spherical solute species, D is given by the Stokes–Einstein equation

$$D = \frac{k_B T}{6\pi\eta R} \tag{6}$$

where k_B is Boltzmann's constant, T is the absolute temperature, η is the viscosity, and R is the (hydrodynamic) radius. For a solid sphere, $D \sim M^{-1/3}$.

Many particle species of analytical interest are not spheres. For rigid ellipsoids, the Perrin correction factors relate D, D_r, and the lengths of the principal axes. (For a thorough treatment of these and related hydrodynamic issues, see Reference 11, especially Chapters 10–12, 18, and 19.) However, careful studies on species of known shape and size (notably tobacco mosaic virus) suggest that the Perrin factors are not reliable at better than the 10% level (*14*). Inferring particle shape from D and D_r is not highly reliable. For dilute monodisperse polymers in good solvents, the correlation between D and molecular weight M is well established, namely $D = a_D M^{-0.6}$ (*15*). Inferring M of a well-fractionated polymer from $C(t)$ and D, if appropriate standards are employed to determine a_D, is reasonably reliable.

Multicomponent systems

A common analytical problem is the determination of the molecular weight or size distribution of a mixture of homologous polymers. For a dilute N-component mixture, $C(\delta t)$ is a sum of exponentials, one exponential for each component:

$$C(t) = \left[\sum_{i=1}^{N} A_i \exp(-D_i k^2 t)\right]^2 + B \tag{7}$$

In this equation A_i and D_i are the scattering intensity and diffusion coefficient of component i. Equation 7 is often put into integral form. Here $\sum_i A_i = 1$; the relative values of the A_i are said to give the distribution of diffusion coefficients in the sample. (Replacing the A_i with a continuous $A(D)$ gives a more concise, but mathematically more formidable, integral description of $C(t)$; see Reference 16 for details.)

Suppose that one knew that one's data were described by Equation 7. How could the spectrum be analyzed? An effective approach is to fractionate the sample and measure D_i and A_i of each purified component. For example, Loewenstein and Birnboim (*17*) have shown that one can fractionate a sample by layering it onto a transparent ultracentrifuge tube, spinning to separate fractions into vertically resolved horizontal bands, transporting the tube to a light scattering spectrometer, and recording the spectrum of each fraction.

The same procedure should be effective with a gel permeation chromatography (GPC) apparatus and fraction collector, if the GPC apparatus does not dilute the fractions to concentrations too low to be studied with QELSS. Unfortunately, the time required to obtain a reasonable spectrum of many materials (5–15 min) typically makes it difficult to use QELSS (laser beam detector plane aligned to be perpendicular to the direction of flow) as a high-resolution probe on a flow-through chromatographic output. Post-separation QELSS studies of column fractions typically are more effective.

Although fractionation can be inconvenient, a direct mathematical analysis of Equation 7 may be effective. Consider Equation 5. For a monodisperse system, a semilog plot of $C(t) - B$ gives a straight line. The same plot, applied to the spectrum of a mixture, gives a smooth curve. A possible approach is to do linear least-squares fits of the smooth curve to a polynomial

$$0.5 \log (C(t) - B) \approx \sum_{n=0}^{N} K_n(-t)^n/n! \tag{8}$$

The sum over n is a truncated cumulant expansion. (The use of cumulants in light scattering spectroscopy was proposed by Koppel [*16*].) The K_n are the cumulants or central moments; N is the truncation order. For $N = \infty$ the expansion is exact in that every well-behaved sum of exponentials can be written as an infinite cumulant expansion.

The low-order cumulants have simple physical interpretations. The first cumulant is $K_1 = \langle D \rangle k^2$; it gives the light scattering intensity weighted diffusion coefficient. If the diffusing species all have the same optical polarizability, and if they are all much smaller than a light wavelength in size, K_1 gives the z-average (molecular weight squared weighted average) diffusion coefficient D. The second cumulant, K_2 (often expressed as the variance which is $100\sqrt{K_2}/K_1$), provides a value for the range of diffusion coefficients present in the sample. The larger K_2 is, the wider the distribution can be inferred to be. Specifically,

$$K_2 = \sum_{i=1}^{N} A_i(D_i - \bar{D})^2 \tag{9}$$

K_2 is not a measure of the quality of the spectrum in the sense that S/N measures how good a spectrum is. A large K_2 or a large variance indicates that the sample is polydisperse (which may be undesirable, if the experimenter had attempted to prepare a monodisperse sample), but a fit giving a large K_2 is a priori as valid as a fit that gives a small K_2. It is extremely difficult to measure cumulants higher than the second with any precision.

In any fitting procedure, an important question is whether the function being fitted matches the data. Because the S/N with QELSS spectra, which are digitally collected, is so large (typically > 500–1000), a plot of the data and the fitting function is not effective. With a reasonable plot the scatter of the data around the fitting function is too small to be seen reliably. An effective alternative is to plot the residuals: the differences, channel by channel, between measured spectra and their calculated forms.

An attractive alternative to the cumulant expansion is a nonlinear least-squares fit of Equation 7 to a sum of exponentials

$$[C(t) - B]^{1/2} = \sum_{i=1}^{N} A_i \exp(-D_i k^2 t) \tag{10}$$

This format allows computation of the individual A_i and D_i from $D(\delta t)$. With the use of powerful desktop computers, it is not difficult to make a nonlinear least-squares fit unless the number of fitting parameters is extremely large.

Unfortunately, multiexponential fits and data inversions do not work, at least with anything like the precision apparent in the original spectra. The basic difficulty is that sums of exponentials look a great deal alike. The problem is fundamental and mathematical rather than physical in origin. Extracting the A_i and D_i from Equation 10 is an inverse Laplace transform. Inverse Laplace transforms have the mathematical property of being ill-posed problems, a topic on which there

is an extensive literature (*18*). Ill-posed problems are extremely sensitive to noise in the initial data. Even a small amount of noise in $C(t)$ creates a large inaccuracy in the computed A_i. For the inverse Laplace transform, if $C(t)$ could be measured with perfect accuracy, there would be no difficulty in calculating the A_i. With a real $C(t)$ measured with finite precision, an inverse of $C(t)$ often gives a poor estimate of the A_i.

How many data are present in a QELSS spectrum? A thorough discussion of the insensitivity of QELSS to detailed values of the A_i was presented by Pike et al. (*19*), who calculated the S/N needed to do a reliable M-exponential fit, with the helpful constraint that the A_i are nonzero outside of a factor of 5 range of D. A fit was defined to be reliable if it was consistent with M exponentials but was not consistent with $M - 1$ or $M + 1$ exponentials. With this constraint, a reliable two-exponential fit requires $S/N = 10^3$, whereas a reliable three-exponential fit requires $S/N = 10^6$. Of course, a very wide distribution of exponentials will have D_i values spread over more than a fivefold range, so a very wide distribution of D can be fit accurately with more than two exponentials. The work of Pike et al. (*19*) suggests that an $A(D)$ that covers 2 orders of magnitude in D can, at $S/N = 10^3$, be fit reliably by roughly four exponentials.

Pike et al. also emphasize that noise in the data leads to noise in the fit validation parameters (root mean square [rms] error, quality parameter) used to choose the best fit to the data (*19*). Noise in the fit validation parameters restricts one's ability to distinguish which description of the spectrum (which set of A_i values) is the most accurate. Any data set has associated with it some intrinsic level of noise. If two different functions both fit a data set to within the data set's intrinsic noise level, the fact that one fitting function gives a better rms error (or quality parameter) than the other fitting function has no significance. All functions that fit the data to within the data's intrinsic noise level are equally valid; the data do not distinguish among them.

To show how much information is present in light scattering spectra, theoretical spectra for a series of polymer solutions have been calculated and fit to cumulant expansions (*20*). Typical results extracted from a study of some 125 000 Monte Carlo generated spectra appear in the box at right. Solutions had nominal log-normal molecular weight distributions of various M_w/M_n, and polymer chains were assumed to have $D \sim M^{-1/2}$ and scattering power $I \sim M^1$. Random noise was superposed on the computed noise-free spectra. S/N was defined to be the ratio of the random noise (approximated as having equal amplitude in every channel) to $C(0)$, and $S/N = 500$ was selected. This value of S/N represents those that can be attained using a large laser, moderately dilute polymer solution, and nonheroic integrating times (~ 0.5 h). For each value of M_w/M_n 100 sets of random noise were generated, so each of the values in the box is an average over fits to 100 independent spectra of the same notional sample.

With $M_w/M_n = 1.05$, spectra are described to within the noise by one cumulant: A single exponential fit is entirely adequate. At $S/N = 500$, QELSS cannot distinguish between this narrow (but commercially available for some species) molecular weight distribution and a hypothetical, perfectly monodisperse system. Even with M_w/M_n as large as 1.5, only two cumulants are needed to represent the complete spectrum to within the noise. The statement that "only two cumulants are needed" does not imply that one cannot fit the spectra to a series that uses three, four, or eight cumulants. An eight-cumulant numerical fit, made to data for which only two cumulants are needed, will yield eight cumulants, none of which are reliable. Only two cumulants of data were originally present in the data, so the eight-cumulant fit yields two parameters' worth of physical data, mixed nonlinearly with six numbers that characterize the random noise in the spectrum.

Figure 3 shows a polymer molecular weight distribution curve obtained from a high-resolution size-exclusion chromatography (SEC) apparatus with multiple simultaneous output detectors (*21*). The sample had $M_w/M_n \approx 1.50$, approximately matching the final value in the box. Whereas two cumulants are all that can be obtained from the spectrum of this system, a reason-

No. of cumulants required to describe spectra of polymer solutions with log-normal MW distributions, for spectra with $S/N = 500$.

M_w/M_n	Cumulants
1.05	1
1.12	2
1.20	2
1.52	2

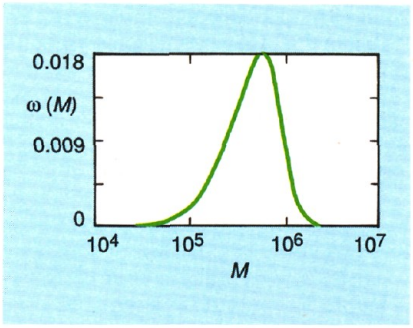

Figure 3. Size-exclusion chromatogram (with multiple simultaneous output detection) of a dextran in water. M_w/M_n for the dextran ~ 1.5 (*21*, *22*).

able estimate (*22*) is that instrumental resolution requires at least eight independent numbers to describe the central part of the SEC curve: one number for each of a series of eight molecular weight regimes. QELSS thus gives much less data about a molecular weight distribution than does a state-of-the-art SEC instrument. In particular, because QELSS of a system with this $M(w)$ and $S/N = 500$ only provides two reliable cumulants, the skewedness of $M(w)$ evident in the SEC data would not be observable with QELSS.

Complications and artifacts

The previous discussion emphasized the requirement that solutions be dilute. At elevated solute concentrations, diffusing particles interact with each other, modifying the diffusion coefficients. Interpreting light scattering spectra of nonideal (concentrated) solutions involves substantial complications. First, in nondilute solutions there are two physically distinct translational diffusion coefficients. One of these, the self or tracer diffusion coefficient D_s, effectively measures the diffusion of an identifiable, labeled particle through a uniform background of unlabeled, unseen particles. The other diffusion coefficient, the mutual diffusion coefficient D_m, describes the relaxation of a concentration gradient. D_s can be measured by such techniques as fluorescence recovery after photobleaching and pulsed field gradient NMR. QELSS and classical gradient diffusion techniques both determine D_m.

D_s and D_m have different dependencies on concentration. D_s almost always falls with c. For example, for random-coil polymers in good and theta solvents, the relation $D_s = D_0 \exp(-\alpha c^{\nu})$ is generally followed to good approximation at all c; α and ν are polymer-dependent scaling coefficients (*23*). In contrast, at large c, D_m may either increase or decrease, perhaps by factors of 2 or 3 relative to the low-concentration limit. In some cases, unsurprisingly, D_m is therefore relatively independent of c. However, an observed concentration independence of D_m has no fundamental significance.

It is certainly not correct to assume that D_m is independent of c and then use the Stokes–Einstein equation and D_m measured at high concentration to calculate a particle radius. An observed independence of D_m and c could arise, for example, from countervailing changes in particle size and interparticle interactions. If one does not keep careful track of the techniques used to measure different values for D, confusion may result. (See Reference 24 for a detailed discussion.)

By extrapolating measurements to the limit of low-solute concentration, artifacts resulting from concentration effects usually can be avoided. For typical globular solutes, at concentrations below 10–30 mg/mL, D_m does not have a strong dependence on concentration. For random-coil polymers, to have a dilute solution the mean distance between polymer chains must be substantially larger than the radius of gyration; concentrations below 1–2 mg/mL are usually acceptable. In some systems D_m has a high-concentration plateau regime, so one can find a D_m that appears to be independent of c but that does not equal the Stokes–Einstein equation D. Polyelectrolyte systems introduce particular difficulties because polyelectrolyte solutions that contain little or no added background electrolyte have odd physical properties. At salt concentrations above 0.1 M, these odd properties are largely abolished. Even at high salt concentration, D of a polyelectrolyte system generally depends on the polyelectrolyte concentration.

A ternary system of practical interest incorporates a solvent, a weakly scattering macromolecular species (whose concentration may be very large), and an intensely scattering dilute probe species. If the probe species dominates the scattering spectrum, the measured D is essentially the self-diffusion coefficient of the probe. In this special case, combining D with the Stokes–Einstein equation allows one to infer a solution microviscosity—the viscosity that characterizes the resistance of the solution to the diffusion of mesoscopic particles. Even with very large probes, the microviscosity may differ substantially from the viscosity obtained with macroscopic low-shear measurements. (For an example of this technique, see Reference 25.)

A common, difficult-to-recognize artifact stems from multiple scattering,

in which photons are scattered by more than one diffusing particle before reaching the detector. Multiple scattering causes the diffusion coefficient to be artifactually large by factors of 5 or more. Multiple scattering can be rejected as a source of error by working with water-white or faintly lucent samples and by confirming that D does not change when the sample is diluted. Technically it is correct that multiple scattering depolarizes the incident (polarized) laser light; however, the depolarized (VH) spectrum resulting from double scattering is much weaker ($\sim$ 2% as strong) than the conventional polarized spectrum. The near disappearance of the spectrum when one places a horizontal polarizer between the sample and the detector is not a good indicator of the absence of significant multiple scattering effects. The homodyne coincidence spectrometer, a two-incident beam, two-detector instrument in which $C(t)$ is obtained from the cross-correlation between the intensities at the two detectors (*26, 27*), has been described. Because multiple scattering fluctuations are uncorrelated at the two detectors, $C(t)$ from this instrument is not perturbed by multiple scattering artifacts.

The discussion of scattering intensity fluctuations was based on the notion of interference between light scattered by different particles. If a single macromolecule is larger than $\sim \lambda/20$, one also has significant interference between light scattered by different parts of the same macromolecule. Kerker (*8*) and Huglin (*7*) treat intramolecular interference in detail. A major physical consequence of intramolecular interference is that the angular dependence of the intensity of the scattered light is not the same for all species; larger particles scatter preferentially in the forward direction. The D obtained from QELSS is a z-(light scattering intensity weighted) average. If several species are present in the sample and all species do not have the same dependence of scattering intensity on scattering angle, some will tend to dominate the scattering in some directions whereas others will be more important in the spectrum, as seen with other scattering angles. D then depends on scattering angle. In particular, unless rigorous care has been taken to exclude dust and other aggregates from the sample, it is frequently true that D falls sharply with falling scattering angle for near-forward scattering.

Conclusion

QELSS has a variety of important analytical applications. Light scattering spectroscopy directly measures the transport of macromolecules in solution. For dilute species, a translational diffusion coefficient D is obtained. At elevated solute concentrations, D can be identified as the mutual diffusion coefficient D_m.

QELSS is an effective tool for sizing mesoscopic particles and for estimating z-average polymer molecular weights. The technique is directly applicable to monodisperse systems; analysis of polydisperse systems is feasible if the systems are first size-fractionated. With unfractionated polydisperse systems, QELSS provides a rough estimate of the width of the size distribution.

Light scattering spectra of simple fluids (which may require a Fabry–Perot spectrometer instead of a digital correlator to analyze) reveal sound speeds and thermal diffusivities. The noninvasive nature of light scattering makes it especially useful for studying transport in fluids near critical points, where conventional methods are difficult to apply (*28*).

Light scattering spectra of ternary solvent:optically inert solute:dilute optical probe systems determine directly the probe's self-diffusion coefficient D_p. With spherical probes, D_p and the Stokes–Einstein equation give a solution microviscosity.

Interpretation of QELSS spectra can be hindered by artifacts. Of particular importance is the fact that the simple Stokes–Einstein equation (Equation 6) only applies to dilute solutions. At large c, D depends on c in a way that varies from species to species. It is incorrect to use D, as measured in a concentrated solution, to infer a radius R from the Stokes–Einstein equation.

Special problems arise if the scattering species is a polyelectrolyte. These difficulties are reduced but not eliminated if the solvent has a large (0.5 M or higher) ionic strength.

It is very easy to overanalyze data. By using methods that are formally valid when no noise is present, one can readily obtain more parameters from a QELSS spectrum than are actually supported by the data. This artifact sometimes becomes apparent if one compares analyses of a half-dozen spectra of the same sample.

References

(1) Phillies, G.D.J. In *Treatise on Analytical Chemistry*; Elving, P. J., Ed.; John Wiley & Sons: New York, 1986; Part I, Vol. 8, p. 1.
(2) Phillies, G.D.J. *J. Appl. Polym. Sci.* **1989**, *43*, 275.
(3) Chu, B. *Laser Light Scattering*; Academic: New York. 1974.

(4) Berne, B. J.; Pecora, R. *Dynamic Light Scattering with Applications to Chemistry, Biology, and Physics*; Wiley-Interscience: New York, 1976.
(5) *Photon Correlation and Light Beating Spectroscopy*; Cummins, H. Z.; Pike, E. R., Eds.; Plenum: New York, 1974.
(6) *Photon Correlation Spectroscopy and Velocimetry*; Cummins, H. Z.; Pike, E. R., Eds.; Plenum: New York, 1977.
(7) *Light Scattering from Polymer Solutions*; Huglin, M. B., Ed.; Academic: New York, 1973.
(8) Kerker, M. *The Scattering of Light and Other Electromagnetic Radiation*; Academic: New York, 1973.
(9) Crosignani, B.; DiPorto, P.; Bertolotti, M. *Statistical Properties of Scattered Light*; Academic: New York, 1975.
(10) Schmitz, K. S. *An Introduction to Dynamic Light Scattering by Macromolecules*; Academic: San Diego, 1990.
(11) Cantor, C. R.; Schimmel, P. R. *Physical Chemistry of Macromolecules*; W. H. Freeman and Company: San Francisco, 1980; Vol. 2, Chapter 14.
(12) Ford, N. C. In *Measurement of Suspended Particles by Quasi-Elastic Light Scattering*; Dahneke, B., Ed.; Wiley: New York, 1983.
(13) Foord, R.; Jakeman, E.; Oliver, C. J.; Pike, E. R.; Blagrove, R. J.; Wood, E.; Peacocke, A. R. *Nature* **1970,** *277*, 242.
(14) Wilcoxon, J.; Schurr, J. M. *Biopolymers* **1983,** *22*, 849.
(15) de Gennes, P. G. *Scaling Concepts in Polymer Physics*; Cornell University Press: Ithaca, 1979; p. 177.
(16) Koppel, D. E. *J. Chem. Phys.* **1972,** *57*, 4814.
(17) Loewenstein, M. A.; Birnboim, M. H. *Biopolymers* **1975,** *14*, 419.
(18) Morozov, V. A. *Methods for Solving Incorrectly Posed Problems*; Springer-Verlag: New York, 1984.
(19) Pike, E. R.; Watson, D.; McNeil-Watson, F. In *Measurement of Suspended Particles by Quasi-Elastic Light Scattering*; Dahneke, B., Ed.; Wiley: New York, 1983.
(20) Phillies, G.D.J. *J. Chem. Phys.* **1988,** *89*, 91.
(21) Callec, G.; Anderson, A. W.; Tsao, G. T.; Rollings, J. E. *J. Appl. Polym. Sci.* **1984,** *22*, 287.
(22) Rollings, J. E., personal communication.
(23) Phillies, G.D.J. *Macromolecules* **1986,** *19*, 2367.
(24) Phillies, G.D.J. *J. Colloid Interf. Sci.* **1982,** *86*, 226.
(25) Phillies, G.D.J.; Inglefield, H.; Kiss, M.; Maclung, D.; Maguire, M.; Malone, C.; Pirnat, T.; Teasdale, N.; Yu, L-P.; Rollings, J. *Macromolecules* **1989,** *22*, 4068.
(26) Phillies, G.D.J. *J. Chem. Phys.* **1981,** *74*, 260.
(27) Phillies, G.D.J. *Phys. Rev. A* **1981,** *24*, 1939.
(28) *Dynamic Light Scattering—Applications of Photon Correlation Spectroscopy*; Pecora, R., Ed.; Plenum: New York, 1985; Chapter 7.

This material is based on work supported by the National Science Foundation under Grant DMR88-11222.

George D. J. Phillies, associate professor of physics at Worcester Polytechnic Institute, received S.B. degrees in physics and in life sciences (1969) and a doctor of science in physics (1973) from Massachusetts Institute of Technology. He pursued postdoctoral studies in the Harvard–MIT Life Sciences Program and the UCLA Chemistry Department. His research interests include light scattering spectroscopy, statistical mechanics, complex fluids, biophysical chemistry, and polymer dynamics.